Two coherent phonon modes at the metal-insulator transition of the spinel $CuIr_2S_4$ compound using femtosecond pump-probe spectroscopy

I. Matsubara,* S. Ebihara, T. Mishina, and J. Nakahara
Division of Physics, Hokkaido University, Sapporo 060-0810, Japan

N. Matsumoto and S. Nagata
Department of Material Science and Engineering, Muroran Institute of Technology, 27-1 Mizumoto-cho, Muroran, Hokkaido 050-8585, Japan

(Received 17 December 2008; published 24 February 2009)

We report an observation of coherent phonons in thio spinel $CuIr_2S_4$ by using femtosecond pump-probe spectroscopy. We found two pronounced and long-lived phonon modes (2.5 and 4.2 THz) superimposed on the electronic response which corresponds to optical excitation from Ir $5d\ t_{2g}$ to e_g. At the metal-insulator transition (230 K), the lifetime of the 2.5 THz phonon mode increases abruptly, whereas the other phonon parameters, including the 4.2 THz phonon mode, show negligible changes. Moreover, we observed the lifetime extension of the 4.2 THz phonon mode attributed to the photoinduced phase transition which is enabled below 100 K. These anomalous phonon behaviors are strongly correlated with a complicated nature of electron-phonon interaction in $CuIr_2S_4$.

DOI: 10.1103/PhysRevB.79.054110 PACS number(s): 78.47.−p, 63.20.K−, 71.30.+h

I. INTRODUCTION

Spinel compounds AB_2X_4 have been studied for many years because they exhibit a large variety of interesting physical properties, including superconductivity, cooperative antiferromagnetism, heavy fermion, charge-ordered state, and spin dimerization. $CuRh_2S_4$ and $CuRh_2Se_4$ (Ref. 1) reveal superconducting transitions between 3 and 4 K. Magnetite Fe_3O_4 shows a ferrimagnetic transition at high temperature (858 K). Fe_3O_4 undergoes a metal-insulator transition (MIT) (the Verwey transition) at 120 K interpreted as a charge-ordering transition of Fe^{2+} and Fe^{3+} on the B sites.[2] Among various spinel compounds $CuIr_2S_4$ is well known for the first-order MIT at T_{MIT} of 230 K.[3] The transition is characterized by the sudden increase in the electrical resistivity, disappearance of Pauli paramagnetism, and lowering of structural symmetry. The Pauli paramagnetic behavior is observed in the metallic phase, whereas the insulating phase shows almost temperature-independent diamagnetic behavior.[4,5] According to NMR measurements, x-ray photoemission spectroscopy,[6] and band calculation,[7] the Cu ion is in a monovalent state and the effective valence of Ir is 3.5+ in the metallic phase. At the MIT, $Ir^{3.5+}$ ions are charge ordered and separated into Ir^{3+} and Ir^{4+} ions. Ir ions are found in two electrically different states Ir^{3+} and Ir^{4+} with equal populations. $Ir^{4+}(s=1/2)$ ions are found to form structural dimers. Lattice structure has been also investigated. From the x-ray diffraction measurements, $CuIr_2S_4$ has been found to possess a normal cubic structure in the high-temperature metallic phase. In the first report of the powder x-ray experiment, the diffraction pattern for the insulating phase was approximated by the tetragonal structure.[5] High-resolution x-ray experiments[8,9] and transmission electron microscopy[10] have shown triclinic distortion with the spin dimerization of the Ir^{+4} ion in the insulating phase. The transition is accompanied by volume reduction by about 0.7%.

Although lattice structure and distortion have been intensively investigated by x-ray experiments, there has been no report on the lattice vibration. Moreover, the information on the photoexcited state and the knowledge of the electron-phonon dynamics in the vicinity of the phase transition are quite restricted. In this paper, we report on the femtosecond pump-probe study of the temperature dependences of the lifetimes and frequencies of coherent phonons in $CuIr_2S_4$. We found anomalous temperature dependences of lifetimes of the phonons and clarified the close relationship between these anomalous phonon behaviors and phase transitions in $CuIr_2S_4$.

II. EXPERIMENT

Single crystals $CuIr_2S_4$ were grown by a self-flux method,[11] and the (100) surface was used for the time domain reflectivity measurements. The sample was placed into vacuum on a cold finger of a liquid He cryostat. Time-resolved optical reflectivity was measured with the use of a pump-probe technique on the (100) surface at various temperatures. A mode-locked Ti:sapphire laser produces 130 fs pulses at a repetition rate of 80 MHz with a wavelength centered at 790 nm. The pulses were divided into pump and probe beams. To obtain the time-resolved reflection spectrum, the time delay of the probing pulse was varied by using a sliding retroreflector. The polarization of the pump beam was rotated by 90° with the use of a half-wave plate so that the polarizations of the pump beam were set to be perpendicular to the probe beam. They were focused on the sample surface in diameter of about 10 μm. We used a 10 mW pump power and a 3 mW probe power. The reflectivity change was measured as a function of time delay. In order to emphasize the oscillatory part of the signals, we performed a time modulation technique. The delay between the pump and probe pulses was modulated by a shaker at a frequency of 80 Hz, and oscillation components of the intensity of the reflected probe beam were detected by a lock-in amplifier.

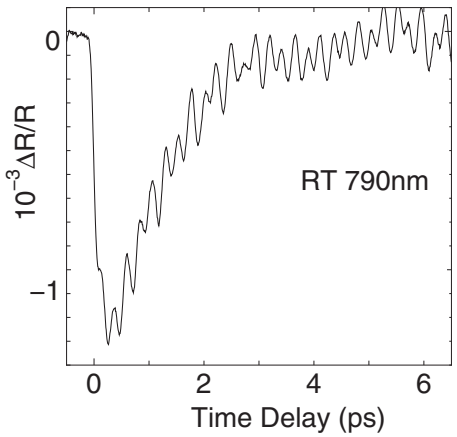

FIG. 1. The time-resolved reflectivity for $CuIr_2S_4$ at room temperature. The intensities of the pump and probe beams are 10 and 3 mW, respectively. The center wavelength of the laser is 790 nm. Reflectivity decreases on irradiating laser pulse and shows single exponential decay with a lifetime of 1.5 ps. The oscillatory structure is superimposed on the single exponential component.

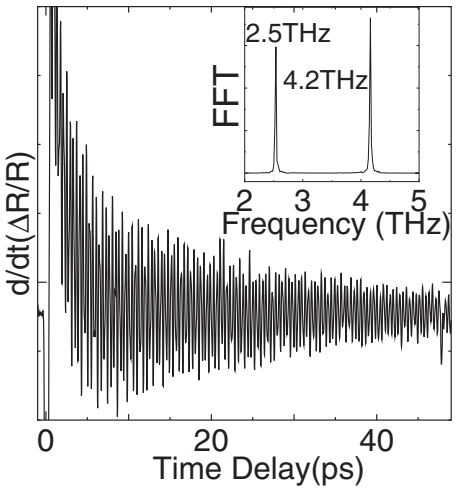

FIG. 2. Time derivative of the reflectivity change corresponds to Fig. 1. Inset shows the Fourier transformation of the time derivative data. The frequencies of the oscillation components are 2.5 and 4.2 THz. The lifetimes of these modes are very close and about 20 ps.

III. RESULTS AND DISCUSSION

The typical time-resolved reflectivity change at room temperature is shown in Fig. 1. When the laser pulse is irradiated ($t=0$), the reflectivity promptly decreases. Then the time-resolved reflectivity change shows a monotonically increasing component (electronic response) and two oscillation components (coherent phonons). The reflectivity signal corresponds to an optical transition from Ir $5d$ t_{2g} to e_g band, comparing the laser wavelength in our experiments with the optical conductivity spectrum,[12,13] and we confirmed the resonant enhancement of the electronic response when the laser wavelength approaches a band-gap energy (600 nm, Ir $5d$ $t_{2g} \sim e_g$).[13]

To investigate the fine structure of the oscillation components of the time-resolved reflectivity, time derivatives of the reflectivity change were measured as a function of time delay at room temperature and shown in Fig. 2. The Fourier transformation of the time domain data is shown in the inset of Fig. 2. Two sharp peaks are located at 2.5 and 4.2 THz.

Both coherent phonons (2.4 and 4.2 THz) in $CuIr_2S_4$ behave as a cosine function. This behavior shows that these phonon modes are generated by a displacive excitation of coherent phonon (DECP) mechanisms.[14] In DECP, the optical excitation by pump pulse makes the atoms move toward a different equilibrium position of the excited state, which then triggers coherent phonons to oscillate. Therefore our coherent phonon signals are related to the real carrier generation and the successive change in the equilibrium position of atoms.

Time-resolved reflectivity change at temperatures of 300 and 30 K are shown in Fig. 3(a). At 300 K (metallic phase), the electronic response shows almost single exponential decay with a lifetime of 1.5 ps, whereas the signal at 30 K (insulator phase) shows a long decay component in addition to the rapid exponential decay. We fitted the temperature dependence of the electronic response using the following equation and determined the relaxation rate of the rapid decaying component (γ) and the intensity of the long decaying component (B),

$$(\Delta R/R)_{\text{electron}} = A_e \exp(-\gamma t) + B. \quad (1)$$

A_e is about 10^{-3} and the temperature dependence is negligible compared to the other experimental dependences. Figure 3(b) shows the temperature dependences of relaxation rate (γ) of the rapid decaying component and the intensity of the long decaying component (B) normalized by its peak value at 150 K. The relaxation rate of the rapid decaying component shows a slight and gradual temperature change which is explained by the suppression of phonon scattering at low temperatures, whereas the clear long decaying component emerges below the MIT temperature.

Below the MIT, the ground state t_{2g} is split into two subbands with spin dimerization, whereas the change in the

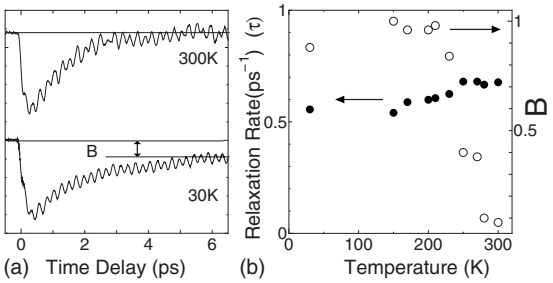

FIG. 3. (a) The time-resolved reflectivity changes at temperatures of 300 and 30 K. At 30 K (insulator phase), the long decaying component indicated by B emerges. (b) Closed circles show the relaxation rate of the rapid decaying component (γ). Open circles show the intensity of the long decaying component (B). The intensity of the long decaying component (B) normalized by its peak value at 150 K. The relaxation rate of the rapid decaying component (γ) decreases as temperature is decreased. The intensity of the long decaying component indicated by B develops below the MIT temperature.

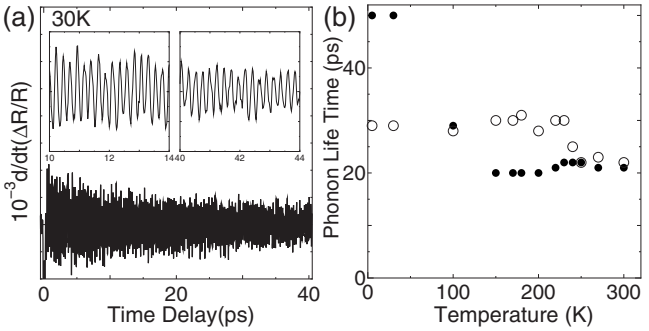

FIG. 4. (a) Time derivative of reflectivity change at 30 K. Insets show time derivative of the horizontally magnified data for the time intervals of 10–14 and 40–44 ps. (b) Temperature dependence of phonon lifetime. Closed circles show the 4.2 THz mode and open circles show the 2.5 THz mode. The lifetime of the 2.5 THz mode steplike increase at the MIT temperature. The lifetime of the 4.2 THz mode is changed gradually about 100 K.

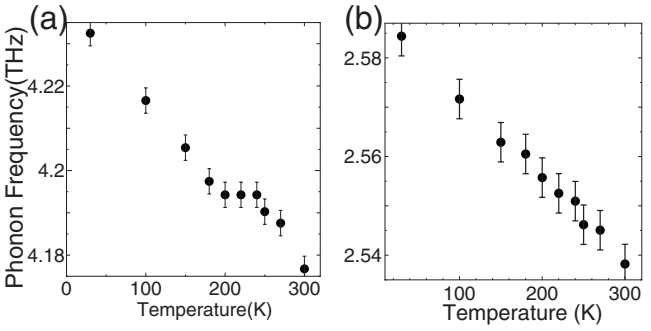

FIG. 5. (a) Temperature dependence of phonon frequencies of the 4.2 and (b) 2.5 THz modes. These frequencies get higher slightly as temperature is decreased. Temperature coefficients of the phonon frequencies are about -5×10^{-5} (1/K).

excited-state e_g band is negligible. Considering the change in the electronic states below the MIT, the relaxation of the carrier is assigned to intraband carrier cooling in the excited state e_g and the origin of the long decaying component is attributed to the reconfiguration of the ground states t_{2g}.

To investigate the temperature dependence of coherent phonons, the time derivative of reflectivity was also measured at various temperatures. Since the lifetimes of the coherent phonons are very long, we employed the following procedure to estimate the lifetimes of the coherent phonons. The change in amplitude within a short time interval is negligible; therefore we fitted the experimental data for 4 ps intervals at specified time delays using the following equation:

$$\frac{d}{dt}\left(\frac{\Delta R}{R}\right) = A_L \sin(\omega_L t) + A_H \sin(\omega_H t), \tag{2}$$

where A_L, A_H, ω_L, and ω_H are amplitudes and frequencies of the 2.5 and 4.2 THz modes, respectively. We plotted the averaged amplitudes versus the time delays and obtained the lifetime. The time derivative of reflectivity at 30 K is shown in Fig. 4(a). Insets show horizontally magnified signals in the time intervals of 10–14 and 40–44 ps. Temperature dependences of phonon lifetimes of 2.5 (open circles) and 4.2 THz (closed circles) modes are shown in Fig. 4(b). The lifetime of the 2.5 THz mode shows a flat temperature dependence and a step-function-like change at the MIT temperature. The lifetimes of the 4.2 THz mode is almost constant above 120 K.

There are basically two mechanisms for determining the lifetimes of phonons: one is the phonon-phonon interaction and the other is the carrier-phonon interaction. In the phonon-phonon interaction the optical mode decays into two low-frequency phonons satisfying the conservation of energy and crystal momentum (decay channel) via anharmonicity in the lattice potential. The phonon-phonon interaction has temperature dependence through the Bose factor.[15] In our case, phonon-phonon interaction should strongly depend on temperature around 230 K since the thermal energy is larger than the phonon energies. However, the experimental result shows flat temperature dependence and it indicates that phonon-phonon interaction gives minor contribution to the decay process of these optical phonon modes. In the carrier-phonon interaction the decay rate of phonons is proportional to the carrier density. The carrier density dependence of the lifetime of the phonons in GaN has been reported, and A_1 and E_2 modes show the different carrier density dependences there.[16] In $CuIr_2S_4$, the carrier density decreases at the MIT temperature; therefore, the carrier-phonon interaction is more likely to explain the lifetime expansion of the 2.5 THz phonon mode. On the other hand, the negligible change at 230 K in the lifetime of the 4.2 THz mode is explained by the weak-coupling constant to the carrier compared with the 2.5 THz mode as expected from the GaN case.

The lifetime of the 4.2 THz mode increases gradually around 100 K. At 20 K, the lifetime of the 4.2 THz mode reaches up to 50 ps which is two times as much as the lifetime at room temperature. This lifetime corresponds to the spectral width with 0.7 cm^{-1} which is very difficult to approach by conventional Raman spectroscopy measurements. The reason for the lifetime increase in the 4.2 THz mode around 100 K is quite marvelous. There are some reports on phase transition in $CuIr_2S_4$ around this temperature range. Furubayashi *et al.*[17] demonstrated that the resistance decreases drastically and the symmetry changes from tricrinic to tetragonal by x-ray irradiation at low temperatures ($T \leq 100$ K). Recently Tsujimoto *et al.*[18] and Takubo *et al.*[19] indicated photoinduced phase transition around this temperature by irradiating 532 nm light similar to the case of x-ray. In our case, 790 nm laser irradiation causes the same phase transition and the lifetime expansion is attributable to this phase transition.

Temperature dependences of phonon frequencies are shown in Fig. 5. As temperature decreases, frequencies of both phonon modes slightly increase. No anomaly appears at the MIT temperature within our experimental accuracy. Temperature coefficients of the phonon frequencies are about -5×10^{-5} (1/K) which is the same order as in the case of conventional semiconductorlike silicon. Since the magnitudes of the anharmonicity are very close to the semiconductors, the minor contribution of the phonon-phonon interaction is explained by the lack of decay channels of these modes.

IV. CONCLUSION

In conclusion, we carried out the femtosecond pump-probe measurements in $CuIr_2S_4$. Time domain reflectivity change is investigated at various temperatures. We observe electronic response which corresponds to the optical transition from Ir $5d$ t_{2g} to e_g. We found two coherent phonon modes (2.5 and 4.2 THz) in $CuIr_2S_4$. They show temperature-induced anomalous behaviors. Although these phonon frequencies (2.5 and 4.2 THz) do not abruptly change at the MIT temperature (230 K), the lifetime of the 2.5 THz mode shows step-function-like change attributed to the MIT carrier reduction. Moreover, the 4.2 THz mode reveals the unexpected expansion of lifetime around 100 K, which is explained by the photoinduced phase transition. Further experimental and theoretical studies are needed to understand the electron-phonon dynamics below 100 K in $CuIr_2S_4$. Our results demonstrate that pump-probe spectroscopy is a powerful tool to investigate electron-phonon dynamics in strongly correlated electron systems.

*ichirou@phys.sci.hokudai.ac.jp

[1] T. Hagino, Y. Seki, N. Wada, S. Tsuji, T. Shirane, K. I. Kumagai, and S. Nagata, Phys. Rev. B **51**, 12673 (1995).
[2] M. Imada, A. Fujimori, and Y. Tokura, Rev. Mod. Phys. **70**, 1039 (1998).
[3] S. Nagata, T. Hagino, Y. Seki, and T. Bitoh, Physica B **194-196**, 1077 (1994).
[4] H. Suzuki, T. Furubayashi, G. Cao, H. Kitazawa, A. Kamimura, K. Hirata, and T. Matsumoto, J. Phys. Soc. Jpn. **68**, 2495 (1999).
[5] T. Furubayashi, T. Matsumoto, T. Hagino, and S. Nagata, J. Phys. Soc. Jpn. **63**, 3333 (1994).
[6] J. Matsuno, T. Mizokawa, A. Fujimori, D. A. Zatsepin, V. R. Galakhov, E. Z. Kurmaev, Y. Kato, and S. Nagata, Phys. Rev. B **55**, R15979 (1997).
[7] T. Oda, M. Shirai, N. Suzuki, and K. Motizuki, J. Phys.: Condens. Matter **7**, 4433 (1995).
[8] H. Ishibashi, T. Sakai, and K. Nakahigashi, J. Magn. Magn. Mater. **226-230**, 233 (2001).
[9] P. G. Radaelli, Y. Horibe, M. J. Gutmann, H. Ishibashi, C. H. Chen, R. M. Ibberson, Y. Koyama, Y. S. Hor, V. Kiryukhin, and S. W. Cheong, Nature **416**, 155 (2002).
[10] W. Sun, T. Kimoto, T. Furubayashi, T. Matsumoto, S. Ikeda, and S. Nagata, J. Phys. Soc. Jpn. **70**, 2817 (2001).
[11] N. Matsumoto and S. Nagata, J. Cryst. Growth **210**, 772 (2000).
[12] M. Hayashi, M. Nakayama, T. Nanba, T. Matsumoto, J. Tang, and S. Nagata, Physica B **281-282**, 631 (2000).
[13] N. L. Wang, G. H. Cao, P. Zheng, G. Li, Z. Fang, T. Xiang, H. Kitazawa, and T. Matsumoto, Phys. Rev. B **69**, 153104 (2004).
[14] H. J. Zeiger, J. Vidal, T. K. Cheng, E. P. Ippen, G. Dresselhaus, and M. S. Dresselhaus, Phys. Rev. B **45**, 768 (1992).
[15] C. Aku-Leh, J. Zhao, R. Merlin, J. Menendez, and M. Cardona, Phys. Rev. B **71**, 205211 (2005).
[16] K. J. Yee, K. G. Lee, E. Oh, D. S. Kim, and Y. S. Lim, Phys. Rev. Lett. **88**, 105501 (2002).
[17] T. Furubayashi, H. Suzuki, T. Matsumoto, and S. Nagata, Solid State Commun. **126**, 617 (2003).
[18] A. Tsujimoto, C. Itoh, and H. Ishibashi, The Physical Society of Japan Spring Meeting, Kagoshima, Japan, 2007 (unpublished).
[19] K. Takubo, S. Hirata, J. Y. Son, J. W. Quilty, T. Mizokawa, N. Matsumoto, and S. Nagata, Phys. Rev. Lett. **95**, 246401 (2005).